

Quantum Computer Based Feature Extraction Deep Learning Model for Medical Image Classification

Anish Baral ^a, Shashidhar Ram Joshi ^b

^{a, b} Department of Electronics and Computer Engineering, Pulchowk Campus, IOE, Tribhuvan University, Nepal

✉ ^a076msdsa002.anish@pcampus.edu.np, ^bsrjoshi@ioe.edu.np

Abstract

Medical images are difficult to collect and are expensive full of insecurities. Pandemic such as COVID-19 break out suddenly and may be transferable from one person to another, so we need to identify the victim and isolate them. Presence of less datasets of such cases are difficult for the classical convolution model for prediction of disease. We need a high performance and accurate image classification model that assists doctor in diagnosis. The CNN layer of deep learning is also computationally complex as it needs a lot of weights to train for better performance, this increases the computational complexity of the model. Therefore, it is very necessary to develop a model which is fast, accurate and computationally efficient model. Here, we present a hybrid quantum classical convolution neural network for image classification. This research consists of three hybrid quantum classical model for three different input size images 28*28, 32*32 and 64*64 pixels. We run the model in simulators and different real quantum devices. We found that the hybrid model with less trainable parameters with low resolution and small training images was able to outperform the classical convolution neural network. The best hybrid quantum-classical model in this work was with accuracy of 0.9348 and 12318 trainable parameters. The best classical model was with accuracy of 0.9076. The computationally efficient model was with accuracy of 0.9239 with 2355 learnable parameters.

Keywords

COVID-19, medical image classification, hybrid quantum classical neural networks, quantum convolutional neural networks, quantum computing, image processing

1. Introduction

The coronavirus (COVID-19), which occurred in China in December 2019, quickly spread worldwide and was declared a pandemic by the World Health Organization (WHO) [1]. It is very important to be able to diagnose COVID-19 in an infected patient during an epidemic. To detect COVID-19, it is expected that testing for nucleic acid amplification (NAAT) of the respiratory tract or blood samples will yield positive results using a reverse transcription real-time fluorescence polymerase chain reaction (RT-PCR)[2]. However, due to current clinical experience, the rate of detection and sensitivity is low due to the low viral load in the first stage. Therefore, it is inevitable to give negative results. Otherwise, it can only give good or bad results. The severity and progression of the infection cannot be monitored. It may take 1 day or more to determine the outcome of the test after taking the sample from the patient-ray

the chest is used to detect whether a person has COVID Pneumonia or is normal. Medical imaging technology such as MRI Chest X-ray and CT-Scan also can be used for detection of COVID as the COVID virus affects the lungs section significantly. But the pandemic such COVID-19 availability of higher number of data sets are rare. For building a classical image classification model with greater performance is difficult with such less data set. There should be a image classification model that shows high accuracy in assisting the doctor to diagnose this diseases.

In recent years, there have been major developments in the quantum computing field. Quantum Computing is a hold at the crossroads of computer science and quantum mechanics. It is more powerful than the old computer as it uses quantum bits with two identical regions of old pieces (either 0 or 1). These quantum pieces can have both values at the same time and are commonly referred to as the top provinces. A

computer that I can use these quantum pieces are a quantum computer. Quantum pieces are also called qubits. Provincial assets bring significant benefits to the industry. Two popular quantum algorithm Shor's [3] prime factorization of large integer and Grover's algorithm [4] search of data from large unstructured data. This two algorithm performed the task in few seconds which would take years for the classical computer. There are other works too that the quantum computer performs superior to the classical computer.

Now, researchers are focused on what does the quantum computing offer to the machine learning field. Quantum Eigen vector solver[5], Quantum Support vector machine [6] brought a significant impact in the filed of quantum computing and machine learning. CNN is regarded as the best feature extractor than other neural network model but it has to train a lot of weights and bias. Also, we require a lot of training sets in order to get a perfect CNN model for classification tasks.

Henderson et al. [7] proposed a new image hybrid image classification model that uses feature extraction through the quantum computer that is analogous to the classical convolution layer in CNN. The idea behind Quantum Convolution was similar to the classical convolution, the quantum filter was convoluted over the small subsection of the image and the feature map was obtained in different channels. The process by continued for entire regions of the image. Figure 1 shows the quantum convolution idea in which the feature extraction is done by four qubit quantum circuit and the feature map is obtained over the four channels.

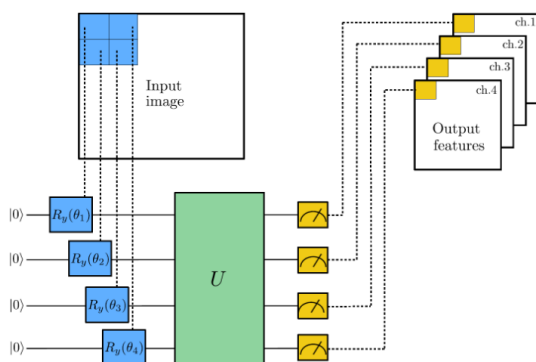


Figure 1: Convolution of classical Image using Quantum Convolution filter

Cong. et al. [8]also proposed Quanvolution Neural Network (QNN) that classified the images using entire quantum computer. This was deep learning model

fully based on quantum computing. In both of these research works introduction of quantum layers in the image classification model improved the performance of the model significantly.

Many researches are done in COVID-19 detection using classical deep learning approach [9, 10, 11]. This main disadvantages of this works were the deep learning model had high computational complexity and required large amount of data sets for model training.

Few works also have been done in COVID-19 detection using Quantum Neural Network. Amin et al. [12]presented a hybrid quantum classical model for COVID-19 detection using chest CT-Scan images. The works consisted of comparison between the classical model and quantum model. The quantum model showed superior classification than the classical model. The limitation behind this model was the image size was of low resolution i. e. 20 * 20 pixels. The classification model only used a single feature extraction 4 Qubits circuit and this work was limited to only binary classification tasks.

Houssien et al. [13] proposed a work in Hybrid Quantum classical network for classification of COVID-19 based on Chest X-ray images. This work used the idea of quantum convolution and other layers were from the classical part. The quantum hybrid model achieved greater accuracy,precision and recall over the classical model. This limitation of this work was ,the classification was only done for 28*28 size input images. The rotation encoding method was only used for classical data to quantum data conversion.

Our work proposes the same quantum convolution idea for hybrid quantum-classical deep learning image classification model. The enhancement of this work are that the classification model was done for other higher dimensional image size 32*32 pixels and 64*64 pixels. Then,the work was compared with the performance of the classical model.

2. Theoretical Background

2.1 Quantum Computing Basics

1. Quantum State Representation: Data in quantum computer can be represented in the form of qubits state. The state of qubits can be represented only by 0 or 1. But,in quantum computing there is certain probability of qubits to be in state 0 and state 1. This simulatneous

existence of a qubit in 0 and 1 state is known as quantum superposition. The fundamental building blocks in quantum computing is called quantum bits or qubits.

A complex vector of size 2 can be used to represent state of qubit as shown below:

$$\begin{bmatrix} \alpha \\ \beta \end{bmatrix} \tag{1}$$

where, α is the probability of qubit to be in state 0 and β is probability of qubit to be in state 1. State 0 in matrix representation is:

$$\begin{bmatrix} 1 \\ 0 \end{bmatrix} \tag{2}$$

State 1 can be represented as:

$$\begin{bmatrix} 0 \\ 1 \end{bmatrix} \tag{3}$$

We can also represent the qubits state by bra-ket notation. The $|\text{ket}_i\rangle$ notation is also called Dirac notation. Thus any arbitrary qubit state in bra-ket notation can be represented as:

$$|\psi\rangle = \alpha|0\rangle + \beta|1\rangle \tag{4}$$

Qubits state could be also represented in Bloch sphere. This representation consists of unit sphere, where south and north poles are placed exponentially. In this representation we can write the general state of qubit as:

$$|\psi\rangle = \cos(\theta/2)|0\rangle + e^{j\psi}\sin(\theta/2)|1\rangle \tag{5}$$

where, θ and ψ lies within whole sphere without any repetitions i.e. $\theta \in [0, \pi]$ and $\psi \in [0, 2\pi]$, θ is latitude and ψ is longitude.

2. Quantum Gates: There are total of 10 quantum gates that acts on single qubits and multi-qubits. The mainly used quantum gates in this research works are:

- Hadamard Gate

Hadamard gate is a single qubit operation gate which takes the qubits in base state and turn them into superposition state. The matrix representation of Hadamard gate is given as:

$$H = \frac{1}{\sqrt{2}} \begin{bmatrix} 1 & 1 \\ 1 & -1 \end{bmatrix} \tag{6}$$

Hadamard operation on state $|0\rangle$ will produce the output $\frac{1}{\sqrt{2}} (|0\rangle + |1\rangle)$ and Hadamard operation on state $|1\rangle$ will produce the output $\frac{1}{\sqrt{2}} (|0\rangle - |1\rangle)$.

The general expression of Hadamard gate on any qubit is given as:

$$H^{\otimes n}|X\rangle = \frac{1}{\sqrt{2^n}} \sum_z (-1)^{X \cdot Z} |Z\rangle \tag{7}$$

This equation can be represented by bitwise inner tensor product of X and Z.

- Rotation Gates

They are single qubits gates that rotates the state of qubits with certain parameters around the basic axes. The general expression for rotation gate is given as:

$$R(\theta, \phi) = \begin{pmatrix} \cos(\theta/2) & -ie^{-i\phi}\sin(\theta/2) \\ ie^{i\phi}\sin(\theta/2) & \cos(\theta/2) \end{pmatrix} \tag{8}$$

Rotation about X-axis (RX) is obtained by putting $\phi = 0$ in general rotation equation. It can be presented as:

$$R_x(\theta) = \begin{pmatrix} \cos(\frac{\theta}{2}) & -\sin(\frac{\theta}{2}) \\ \sin(\frac{\theta}{2}) & \cos(\frac{\theta}{2}) \end{pmatrix} \tag{9}$$

Rotation about Y axis is denoted by (RY) and obtained by putting $\phi = \pi$, represented in matrix form as:

$$R_y(\theta) = \begin{pmatrix} \cos(\frac{\theta}{2}) & -\sin(\frac{\theta}{2}) \\ \sin(\frac{\theta}{2}) & \cos(\frac{\theta}{2}) \end{pmatrix} \tag{10}$$

Rotations about Z-axis is denoted by RZ and can be represented by matrix form as:

$$R_z(\theta) = \begin{pmatrix} e^{-i\theta/2} & 0 \\ 0 & e^{i\theta/2} \end{pmatrix} \tag{11}$$

These gates are used for unitary operation of the qubits.

- Paulies X, Y and Z gates

Pauli X-gate is given in matrix form as:

$$X = |0\rangle\langle 1| + |1\rangle\langle 0| = \begin{bmatrix} 0 & 1 \\ 1 & 0 \end{bmatrix} \tag{12}$$

X-gate switches the state of $|0\rangle$ to $|1\rangle$ and $|1\rangle$ to $|0\rangle$.

Pauli Y-gate is represented in matrix form as:

$$Y = \begin{bmatrix} 0 & -i \\ i & 0 \end{bmatrix} \tag{13}$$

Y-gate switches the state of $|0\rangle$ to $|1\rangle$ and $i|1\rangle$ to $-i|0\rangle$. This gate not only changes the state of qubits but also flips the phase of the qubits.

Pauli Z gate is represented in matrix form as:

$$Z = \begin{bmatrix} 1 & 0 \\ 0 & -1 \end{bmatrix} \quad (14)$$

This gate does nothing changes to $|0\rangle$ state but flips the sign of $|1\rangle$ state to $-|1\rangle$.

3. Quantum Entanglement: Two systems away from each other behaving randomly may be correlated with each other. This phenomenon is called quantum entanglement. Entanglement is done by multi-qubit quantum gate known as Controlled Not (C-NOT). It takes two qubit states as input, one is control bit and another is target bit.

The transformation matrix of C-NOT gate is given by:

$$CNOT = \begin{bmatrix} 1 & 0 & 0 \\ 0 & 1 & 0 \\ 0 & 0 & 1 \\ 0 & 0 & 0 \end{bmatrix} \quad (15)$$

They are used in quantum circuit in order to introduce strong relationship among qubits.

4. Quantum Measurement: Quantum computer being probabilistic in nature cannot give accurate result as the classical computer at one measurement. So, we need to perform several execution and take average of the output value at different shots that is known as expectation value of qubits. Measurement is done in order to study the state of the qubits. The quantum states collapse to classical state during measurement. In our research work measurement is done on the parameterized quantum circuit that is used for quantum convolution. The state of quantum system are changed by the unitary operations by single and multi qubits gates. The Pauli Z gate is used for measurement of quantum state in our research work.

The general expression of expectation value of ϕ state is given by the equation:

$$\langle Z \rangle = \langle \psi | Z | \psi \rangle \quad (16)$$

2.2 Quantum Deep Learning

Significant advancements in the domains of deep learning and quantum computing have been made during the previous few decades. Recently, quantum deep learning and quantum-inspired deep learning approaches have been developed as a result of the growing interest in research at the intersection of the two domains. Benefiting through the advantages of quantum computing shown by Shor's and Grover's algorithm researchers are focused on what would quantum computing offer in the field of machine learning and deep learning. Such a complex architecture in CNN could be replaced by certain quantum circuit or not. Various architecture has been proposed for quantum deep learning such as Quantum Neural Network (QNN), Quantumvolution Neural Network and Quantum RNN.

2.3 Classical Fully Connected Layer

Classical fully connected layer is simply a feed forward neural network present before the output layer in neural network. The output from the convolution layer or pooling layer is flattened and fed into the fully connected layer. The firing of the ANN in fully connected network is as per the formula:

$$g(Wx + b) \quad (17)$$

Where,

x is the input vector,

W is the weight from previous neuron,

b is the bias of neuron and

g is activation function.

This layer consists of maximum number of neurons in the deep learning models and entire features are flattened and they are feed to the neurons. Therefore, computational complexity of the layer is very high as lot of weight has to be trained.

The numbers of trainable parameters in fully connected layers are as follows:

$$Parameters = (n + 1) * m \quad (18)$$

Where, n is the input neuron and m is the output neuron.

2.4 Output Layer

In the output layer we softmax activation function. This function converts numbers vectors in probabilities vector. Each term in the probability vector is related

to the probability of occurrence of each class. The general formula for soft max activation function is:

$$\sigma(z)_j = \frac{e^{z_j}}{\sum_{k=1}^K e^{z_k}} \text{ for } j = 1, \dots, K \quad (19)$$

The fully connected output layer has learnable parameter calculated based on the formula:

$$\text{Parameters} = (n + 1) * m \quad (20)$$

where n is the number of inputs and m is the number of outputs.

3. Methodology

The block diagram of research methodology are given as:

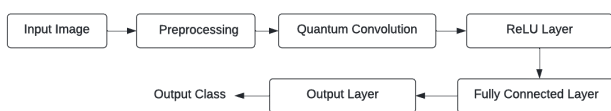


Figure 2: System Block Diagram

3.1 Data Set Description

There was no single dataset of X-ray samples related to COVID-19 so dataset was collected from multiple sources. 1401 COVID-19 samples we recorded from GitHub repository, Radiopaedia, Italian Society of Radiology (SIRM), data repository websites –Figshare. Further 912 images were collected from Mendeley instead of using explicit data expansion techniques. 2313 Pneumonia cases were collected from Kaggle. Finally the dataset was organized into 3 folder (covid, pneumonia, normal) containing chest X-ray posteroanterior (PA) images. Out of 6426 images ,576 were of Covid,1577 of normal and 4273 cases were of pneumonia. The dataset was then splitted into 70% and 30% for training and validation set respectively. Again the same validation set was used for final model testing.

Classes	Training Set	Testing Set
COVID-19	403	173
Normal	1103	474

3.2 System Workflow

Quantum convolution for feature extraction was main focus in this thesis. So the feature were extracted from



Figure 3: Normal Case I



Figure 4: Normal Case II



Figure 5: COVID Case I

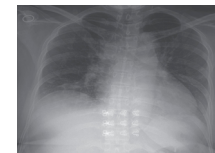


Figure 6: COVID Case II



Figure 7: Pneumonia Case I



Figure 8: Pneumonia Case II

the different qubits of the quantum computer. Since we have limited number of unnoisy qubits we could not feed the whole classical image into quantum computer. So we have used stripe method for feeding the image into the circuit. Various gates were applied which changes the state of the qubits that produces non-linearity. We have also used the phenomenon of superposition and entanglement in order to get benefit from quantum computing. Since, quantum convolution layer have less number of training learnable parameters it could be fitted in between any stage of image classification pipeline in order to reduce computational complexity.

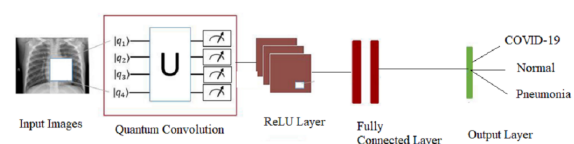


Figure 9: Classification of Image using Quantum convolution and classical fully connected Layer

The various steps performed in this works are mentioned below:

1. The original images were resized into 28*28,32*32 and 64*64 pixels respectively as accordance to the requirement of the experiment.
2. The training images were then normalized by the standard deviation and mean of the training dataset.i.e. $\text{std} = [0.4143, 0.4143,$

0.4143],mean= [0.5160, 0.5160, 0.5160].Random Horizontal Flip was done as part of data augmentation.

3. Quantum convolution is done by taking 2*2 pixels image from top left corner of the image.Rotation encoding technique is applied to convert classical image pixels value into quantum data. The corresponding pixels value rotates the qubits initially at base state to certain state. This step is called step encoding.
4. Then,the parameterized quantum circuit passes through certain unitary operations. The parameterized quantum circuit used for feature extraction is shown in Figure 10. There are five rotational gates that rotates the qubits about certain random parameters. The random parameters are optimized in case of trainable filter where as not optimized in non trainable case.In the quantum circuit there are also three entanglement based CNOT gates,that establish the linkages between the qubits.
5. Then measurement was done on the quantum circuit.Pauli-Z a single qubit gate was used for the measurement purpose. The expectation value of Z in state $|\Psi\rangle$ is given by general formula:

$$\langle Z \rangle = \langle \Psi | Z | \Psi \rangle \quad (21)$$
6. Repeat Steps 3,4 and 5 for entire image to obtain the feature map. The feature map obtained for 28*28 input size image was 14*14,32*32 input size image was 16*16 pixels and 64*64 size input image was 32*32 pixels in four channels respectively.
7. Then ReLU activation is applied after the quantum convolution part in order to introduce non-linearity.
8. The feature map obtained after the quantum convolution is flatten into respective 1D-array. 14*14*4 feature map was flattened into 784 ,16*16*4 into 1024 and 32*32*32 into 4096 1D feature vector respectively.
9. Then, the feature vector passes through classical fully connected layer. Finally, the feature vector is passed to the softmax layer for the output.

10. The weights of fully connected layer and parameters of trainable quantum filter are fine-tuned using optimizers and loss functions. The final stable model is then used for classification.

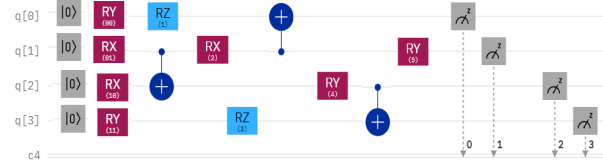


Figure 10: Four Qubits Quantum Convolution Circuit

3.3 Working Environment

1. IBM Quantum Experience
2. Qiskit
3. Google Colab Pro Plus
4. Torch Quantum [14]

4. Result and Discussion

4.1 Experiments

All experiments were performed for same numbers of epochs,learning rate,optimizer and loss function. The hyperparameters used in this works are shown in Table 1. Total 7 experiments were performed in this research works as shown in Table 2. The experiments were varied according to the input image dimension.For each input image dimensional the classical convolution method was also performed for the comparison between the performance of classical filter and quantum filter. In the 1st,2nd and 3rd

No.Epochs	15
Learning Rate	0.0001
Optimizer	Adam
Loss Function	Categorical Cross Entropy

Table 1: Hyperparameters used in this research

experiment the input image size was of 28*28 pixels.We used the filter size of 2*2 and obtained the features map in 4 channels.In first model the classical convolution was applied. In the second model and third model the quantum convolution was applied. The second model had non-trainable quantum filter

Exp. No.	Model No.	Image Size	Filter Size	Filter Type
1	1.1	28 *28	2 *2	Classical
2	1.2	28 *28	2 *2	Non-Trainable Quantum
3	1.3	28 *28	2 *2	Trainable Quantum
4	2.1	32 * 32	2 * 2	Classical
5	2.2	32 * 32	2 * 2	Trainable Quantum
6	3.1	64 * 64	2 * 2	Classical
7	3.2	64 *64	2 * 2	Trainable Quantum

Table 2: Experiments in this research work

and third model had trainable quantum filter. The fourth model and fifth model was for 32*32 input size image with classical and quantum filter respectively. The last two experiments were performed for 64*64 size input images.

4.2 Performance of Model 1.1, Model 1.2 and Model 1.3

From the training accuracy and validation accuracy curve for the three models in this experiment we could find that both training accuracy and validation accuracy of the quantum convolution layer was higher. The accuracy curve of quantum trainable and quantum non-trainable was quite similar. The accuracy curve has converged from epoch 2 in the quantum-classical model the model has converged only from 10th epoch. The best accuracy for model 1.1, model 1.2 and model 1.3 were 0.8129, 0.9289 and 0.9262 respectively. Similarly in the loss curve also the loss of quantum convolution is better than the classical convolution model. The loss curve of trainable and non-trainable filter were similar. The loss curve for quantum filter converge from epoch 4 and epoch 10 for classical filter. The best train loss for model 1.1, model 1.2 and model 1.3 were 0.5311, 0.2851, 0.2737 respectively. The classical model in this experiment had low accuracy and high loss that it makes big errors in most of the data. Accuracy is increased and loss is decreased in case of quantum filter. The quantum filter outperformed the classical filter in terms of test accuracy, precision, recall and F1-score. The summary of classification of each model are listed below:

4.3 Performance of Model 2.1, Model and Model 2.2

Similar to the above experiment the training of quantum filter was more stable than of classical filter. The quantum filter converged at epoch 4 where as the classical filter only converged at epoch 10. The

Model No.	Training Time (Min)	No. of Trainable Parameters	Accuracy	Precision	Recall	F1-Score
1.1	36m 22s	2375	0.7931	0.5833	0.79	0.6233
1.2	142m 39s	2355	0.9239	0.9266	0.9266	0.9033
1.3	212 m 48s	2358	0.9281	0.91	0.93	0.92

Table 3: Model Summary of Model No 1.1, 1.2 and 1.3

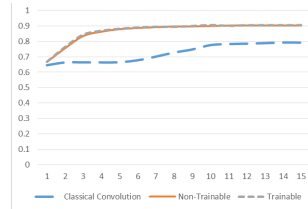


Figure 11: Training Accuracy Curve I

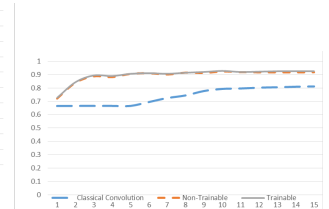


Figure 12: Validation Accuracy Curve I

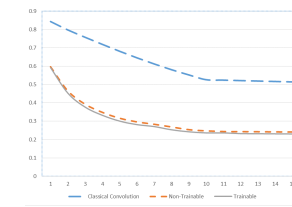


Figure 13: Training Loss Curve I

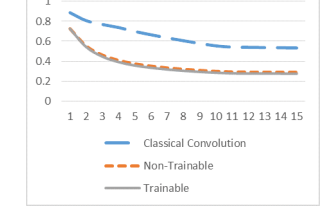


Figure 14: Validation Loss Curve I

quantum filter starts to learn exponentially after epoch 0 but the classical filter start learning properly after epoch 3 and 4. The best train accuracy for the classical convolution was 0.8225 and for the quantum filter was 0.9003. The best train loss for classical model was 0.4866 and for the quantum filter was 0.2801. The accuracy of the classical filter has increased to 28*28 size as it could extract more features from higher dimensional images. As compared to the quantum filter the classical filter accuracy was quite low.

The summary of classification of each model are listed below:

Model No.	Training Time (Min)	No. of Trainable Parameters	Accuracy	Precision	Recall	F1-Score
4.1	37	3102	0.7772	0.59	0.88	0.6566
4.2	296	3082	0.9215	0.8766	0.9266	0.9033

Table 4: Model Summary of Model No 2.1 and 2.2

4.4 Performance of Model 3.1 and Model 3.2

Similar to other experiment the quantum filter started to learn exponentially from the starting epoch and

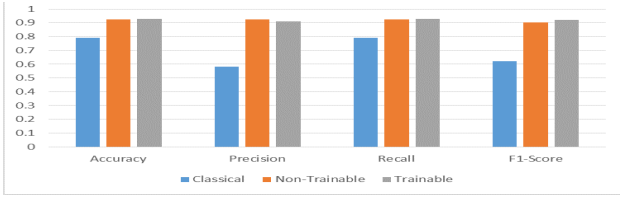


Figure 15: Comparison Metrics between Models I

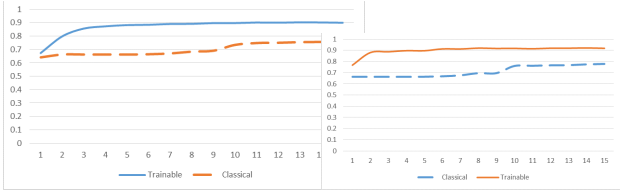


Figure 16: Training Accuracy Curve II

Figure 17: Validation Accuracy Curve II

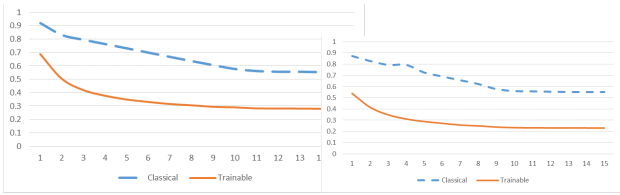


Figure 18: Training Loss Curve II

Figure 19: Validation Loss Curve II

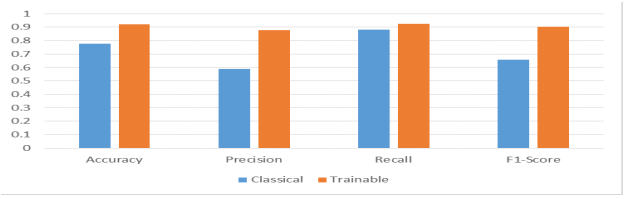


Figure 20: Comparison Metrics between Models II

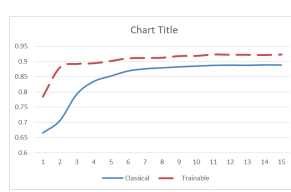


Figure 21: Training Accuracy Curve III

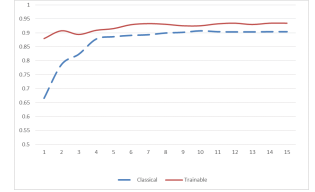


Figure 22: Validation Accuracy Curve II

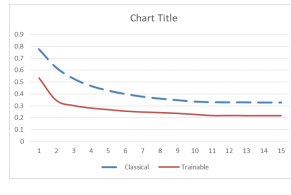


Figure 23: Training Loss Curve III

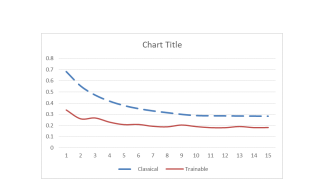


Figure 24: Validation Loss Curve III

converged at 5th epoch where as classical filter also started to train from epoch 0 due to increase of size of image and converged at epoch 7. The accuracy and loss of the classical model was improved significantly in this model and was comparable to quantum filter. The best train accuracy for classical and quantum model was 0.884 and 0.9226 respectively. The best train loss for classical and quantum model was 0.3286 and 0.2176.

The summary of classification of each model are listed below:

Model No.	Training Time (Min)	No of. Trainable Parameters	Accuracy	Precision	Recall	F1-Score
5.1	51	12318	0.9076	0.9	0.9366	0.92
5.2	1157	12298	0.9378	0.85	0.91	0.8833

Table 5: Model Summary of Model No 3.1 and 3.2

4.5 Comparison among Experiments

Among all the performed experiment we could gain insight that quantum filter was able to produce significant accuracy and performance in each experiment. The learn-able parameters of quantum filter was less than of classical. Non-trainable quantum filter produced similar accuracy as the

trainable with fewer number of parameters according to the gradient,so performance of the quantum filter was also good.

The training time of classical model was less as comparable to the quantum model. The quantum model had to be simulated by the local simulator so it increased the training time. Simulating quantum computer in classical increases the complexity exponentially. As the size of image increases training time and number of parameters were also increased.

Model No.	Training Parameters	Training Time(Min)	Accuracy
1.1	2375	36	0.7931
1.2	2355	142	0.9239
1.3	2358	212	0.9281
2.1	3102	37	0.7772
2.2	3082	296	0.9215
3.1	12318	51	0.9076
3.2	12298	1157	0.9348

Table 6: Results of all models

Model 1.3 was evaluated in the real quantum devices as provided by the researchers program by IBM Quantum Experience. The was reservation allowed for five real quantum devices each for 180 minutes per month.1288 test images were tested in each back end. Simulator showed highest accuracy among all devices as it was noise free. IBM also had least CNOT gate error among the five backends so it was able to

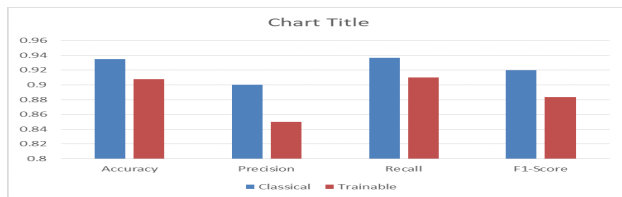


Figure 25: Comparison Metrics between Models III

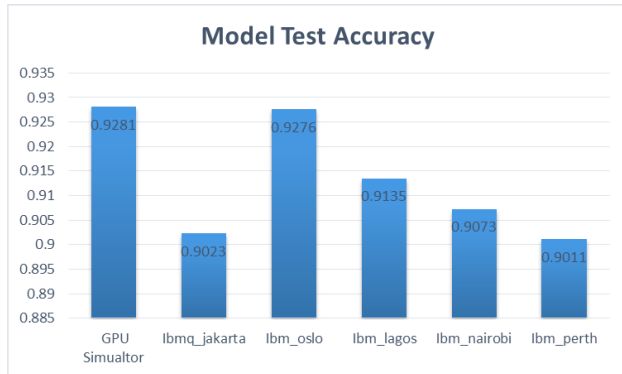


Figure 26: Histogram Showing Model Accuracy in different real quantum devices

achieve highest accuracy among the devices. The accuracy of model in ibmq perth was lowest due high CNOT gate error.

5. Conclusion

The hybrid quantum classical model outperformed all the classical models in all the cases. The non trainable quantum filter showed better performance than the classical convolution filter with less number of trainable parameters. The trainable quantum filter had more accuracy than non trainable filter. The training time of hybrid quantum classical model was more than classical model. The accuracy of model on real quantum devices was low than the simulator due to the CNOT gate error present in each quantum device. The best hybrid quantum model among the experiment was model 3.2 with accuracy of 0.9348 with 12298 trainable parameters. The model with least computational complexity was model 1.2 with 0.9239 accuracy and 2355 trainable parameters.

References

[1] Na Zhu, Dingyu Zhang, Wenling Wang, Xingwang Li, Bo Yang, Jingdong Song, Xiang Zhao, Baoying Huang, Weifeng Shi, Roujian Lu, et al. A novel coronavirus from patients with pneumonia in china, 2019. *New England journal of medicine*, 2020.

[2] V Corman, T Bleicker, S Brünink, C Drosten, O Landt, and M Koopmans. Zambon public health england, m. diagnostic detection of 2019-ncov by real-time rt-rccr incl. *Euro Surveill*, 25:2000045, 2020.

[3] Matthew Hayward. Quantum computing and shor’s algorithm. *Sydney: Macquarie University Mathematics Department*, 2008.

[4] Christof Zalka. Grover’s quantum searching algorithm is optimal. *Physical Review A*, 60(4):2746, 1999.

[5] M Cerezo, Kunal Sharma, Andrew Arrasmith, and Patrick J Coles. Variational quantum state eigensolver. *arXiv preprint arXiv:2004.01372*, 2020.

[6] Amer Delilbasic, Gabriele Cavallaro, Madita Willsch, Farid Melgani, Morris Riedel, and Kristel Michielsen. Quantum support vector machine algorithms for remote sensing data classification. In *2021 IEEE International Geoscience and Remote Sensing Symposium IGARSS*, pages 2608–2611. IEEE, 2021.

[7] Maxwell Henderson, Samriddhi Shakya, Shashindra Pradhan, and Tristan Cook. Quadvolutional neural networks: powering image recognition with quantum circuits. *Quantum Machine Intelligence*, 2(1):1–9, 2020.

[8] Iris Cong, Soonwon Choi, and Mikhail D Lukin. Quantum convolutional neural networks. *Nature Physics*, 15(12):1273–1278, 2019.

[9] Kinshuk Sengupta and Praveen Ranjan Srivastava. Quantum algorithm for quicker clinical prognostic analysis: an application and experimental study using ct scan images of covid-19 patients. *BMC Medical Informatics and Decision Making*, 21(1):1–14, 2021.

[10] Rubina Sarki, Khandakar Ahmed, Hua Wang, Yanchun Zhang, and Kate Wang. Automated detection of covid-19 through convolutional neural network using chest x-ray images. *Plos one*, 17(1):e0262052, 2022.

[11] Emtiaz Hussain, Mahmudul Hasan, Md Anisur Rahman, Ickjai Lee, Tasmi Tamanna, and Mohammad Zavid Parvez. Corodet: A deep learning based classification for covid-19 detection using chest x-ray images. *Chaos, Solitons & Fractals*, 142:110495, 2021.

[12] Javaria Amin, Muhammad Sharif, Nadia Gul, Seifedine Kadry, and Chinmay Chakraborty. Quantum machine learning architecture for covid-19 classification based on synthetic data generation using conditional adversarial neural network. *Cognitive Computation*, pages 1–12, 2021.

[13] Davis Arthur et al. A hybrid quantum-classical neural network architecture for binary classification. *arXiv preprint arXiv:2201.01820*, 2022.

[14] Hanrui Wang, Yongshan Ding, Jiaqi Gu, Yujun Lin, David Z Pan, Frederic T Chong, and Song Han. Quantumnas: Noise-adaptive search for robust quantum circuits. In *2022 IEEE International Symposium on High-Performance Computer Architecture (HPCA)*, pages 692–708. IEEE, 2022.